Journal of Ambient Intelligence and Humanized Computing (2021) 12:7139–7151
https://doi.org/10.1007/s12652-020-02383-3

ORIGINAL RESEARCH

An optimized deep learning network model for EEG based seizure classification using synchronization and functional connectivity measures

G. MohanBabu[1] · S. Anupallavi[1] · S. R. Ashokkumar[1]

Received: 12 November 2019 / Accepted: 21 July 2020 / Published online: 6 August 2020

Abstract
Epilepsy is a brain disorder related to alteration in the nervous system which affects around 65 million people among the world's population. Few works are focused on prediction of seizure relied on deep learning approaches, but the capability of optimal design has no longer been absolutely exploited. This work is focused on the seizure prediction obtained from long-short time records using optimized deep learning network model (ODLN). In this paper, the synchronization patterns and its feasibility of distinguishing the pre-ictal from inter-ictal states are examined by utilizing the interaction graph model as a functional connectivity measure. An optimized deep learning network with short- long-term memory is computed for the prediction of epileptic seizures occurrences. For, the modelling of ODLN, meta-analysis is performed with three modules and memory layers. It is finalized from these results; a two-layer ODLN is optimum to perform the epileptic seizure prediction for four different window sizes from 15 to 120 min. The assessment is implemented on the CHB-MIT Scalp EEG data set, providing 100% sensitivity and low false prediction rate ranges from 0.10 to 0.02 for seizure prediction. The proposed ODLN methodology reveals a notable increase in the performance rate of seizure prediction when compared with existing machine learning and Convolutional neural networks methods.

Keywords Multicast security · Multiple logical key trees · Group key management · One-way key derivation · Rekeying process · False prediction rate · Convolutional neural networks

1 Introduction

Epileptic's seizure is a nervous disorder of the brain which may result in sudden death, fractures, and accidents. Epilepsy can be controlled by therapeutic treatment to some extent. However, intake of antiepileptic drugs (Deckers 2003) fails to reduce the impact of seizures for about 20–30% of affected people. In these conditions, a predominant problem is feasibility of detecting the initial origin of seizure (i.e. pre-ictal) so that to neutralize the invading seizure or confine the injuries during seizures contingency Cui. The classification can be marked out with extracted features from raw EEG signals (Ashokkumar et al. 2019). This method relies on threshold-based approaches. The most reliable predictive features comprise of measured trends from an increase or decrease in the synchronization pattern and phase locking values of EEG signals at the time of pre-ictal state and through complete seizure (Iasemidis et al. 2005).

The synchronization measures so-called, the phase lock value (PLV), the phase lag index (PLI) and the extended PLI as weighted PLI (WPLI) (Vinck et al. 2011) has been utilized. Furthermore, for capturing the real-time variation in the trends of the synchronization pattern, the modified classical indicator has been implemented namely moving average convergence or divergence (MACoD) (Appel 2005). Finally, these features are utilized for seizure prediction algorithm (Deivasigamani et al. 2020). Machine learning (ML) has transfigured the seizure prediction approach for handling the high complexity and volume of EEG data and

✉ G. MohanBabu
[illegible]myubabu@gmail.com

S. Anupallavi
anupallavi1991@gmail.com

S. R. Ashokkumar
srashokkumar1987@gmail.com

[1] Department of Electronics and Communication Engineering, SSM Institute of Engineering and Technology, Dindigul, India

enable the use of multivariate analysis to identify the hidden out characteristics of pre-ictal states (Ramgopal et al. 2014).

In this research work, a graph based methodology is considered for the seizure prediction based on synchronization patterns observed from the EEG signals. Few works are previously performed to prove the interconnection between the synchronization patterns and seizure states (Le Van Quyen et al. 2003; Fisher et al. 2010). The deep learning models are introduced in this work, as optimized deep learning network (ODLN) model for seizure prediction research. This model is an extended work of longer-shorter term memory so-called LSTM architecture (Mormann et al. 2005). For EEG analysis, LSTM network took advantages over the CNN due to its isolating characteristics (Ni et al. 2017). In spite of this advantage, the uses of LSTM for EEG analysis have not acquired the proper attention in seizure prediction. Therefore, deep learning is optimized and this ODLN model has been implemented on the scalp CHB-MIT EEG Database (Cui et al. 2018). The remaining portion of the paper is schematized as follows; Sect. 2 is the depiction of materials and methods, Sect. 3 is the results analysis followed by discussion of results in Sect. 4. Finally, Sect. 5 concludes the workflow of proposed scheme.

2 Materials and methods

2.1 EEG dataset

The EEG record considered in this work was collected from the scalp CHB-MITEEG data set which was recorded from Boston Children's Hospital. It is accessible at PhysioNet. Org. The record consists of 23 paediatric subjects with seventeen females with ages ranges from 1.5–19, males with ages ranging from 3–22 and one missing data intending to analyze their need for surgical involvement. This database is systematized with 24 cases with 256 samples for 1 s using 16-bit resolution. International standard 10–20 electrodes positioning system Shoeb and Guttag (2010) is used for electrode positioning of the electrode. Table 1 provides detailed information about CHB-MIT EEG database.

2.2 Seizure prediction methodology

Seizure prediction approaches generally incorporate two main stages. In the first stage, a number of measures and its indices are extracted from the EEG signal over time so-called feature extraction stage (Hu et al. 2019). The objective of this stage is to reconstruct raw EEG signals into a significant feature that can be exploited to detect the commencement of the seizure (Sathyanarayana et al. 2018). Following up, the classification protocol is assigned to categorize the inter and pre-ictal states Parvez and Paul (2016).

Table 1 An overview of data of the patients present in the CHB-MIT EEG database

Patient id	Age (years)	Gender	No. of seizures	Recordings duration (hh:mm:ss)
Chb_01	11	F	7	40:33:08
Chb_02	11	M	3	35:15:59
Chb_03	14	F	7	38:00:06
Chb_04	22	M	4	156:03:54
Chb_05	7	F	5	39:0[illegible]
Chb_06	1.5	F	10	66:44:0[illegible]
Chb_07	14.5	F	3	67:03:08
Chb_08	3.5	M	5	[illegible]:00:23
Chb_09	10	F	4	67:57:18
Chb_10	3	M	7	50:01:24
Chb_11	12	F	[illegible]	34:47:37
Chb_12	2	F	27	20:41:40
Chb_13	3	F	12	33:00:00
Chb_14	9	F	8	26:00:00
Chb_15	16	M	20	40:00:36
Chb_16	7	F	10	19:00:00
Chb_17	12	F	3	21:00:24
Chb_18	18	F	6	35:38:05
Chb_19	19	F	3	29:55:46
Chb_20	6	F	8	27:36:06
Chb_21	13	F	4	32:49:49
Chb_22	9	F	3	31:00:11
Chb_23	6	F	7	26:33:30
Chb_24	–	–	16	21:17:47
Total			185	979:56:07

The objective of this stage is to accurately hoist an alarm to avoid false positive alarms for the non-pre-ictal period. An outline of the final module of the proposed methodology is portrayed in Fig. 1.

2.3 Synchronizations measure for EEG signals

In this research work, phase-synchronization is computed for EEG signals. This could be measured from the instantaneous phase of the two signals. Synchronization can be measured from the analytical signal. In a real-time series, a(t),the analytical signal is provided as a complex function $z(t) = a(t) + i\hat{a}(t)$ employing Hilbert transforms as provided in Eq. 1:

$$\hat{a}(t) = \frac{1}{\pi} cp \int_{-\infty}^{\infty} \frac{a(\tau)}{t - \tau} d\tau$$

$$a \in L^{q}(R) \quad 1 < q < \infty \tag{1}$$

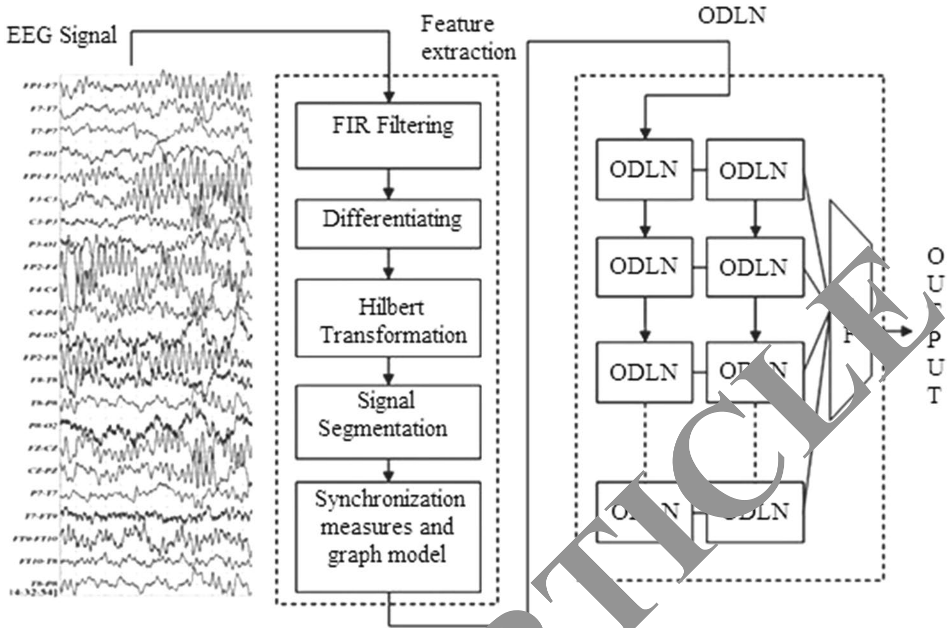

Fig. 1 Diagrammatic representation of the proposed methodology. Extracted features from 5-s long EEG segments are fed into the ODLN for classification

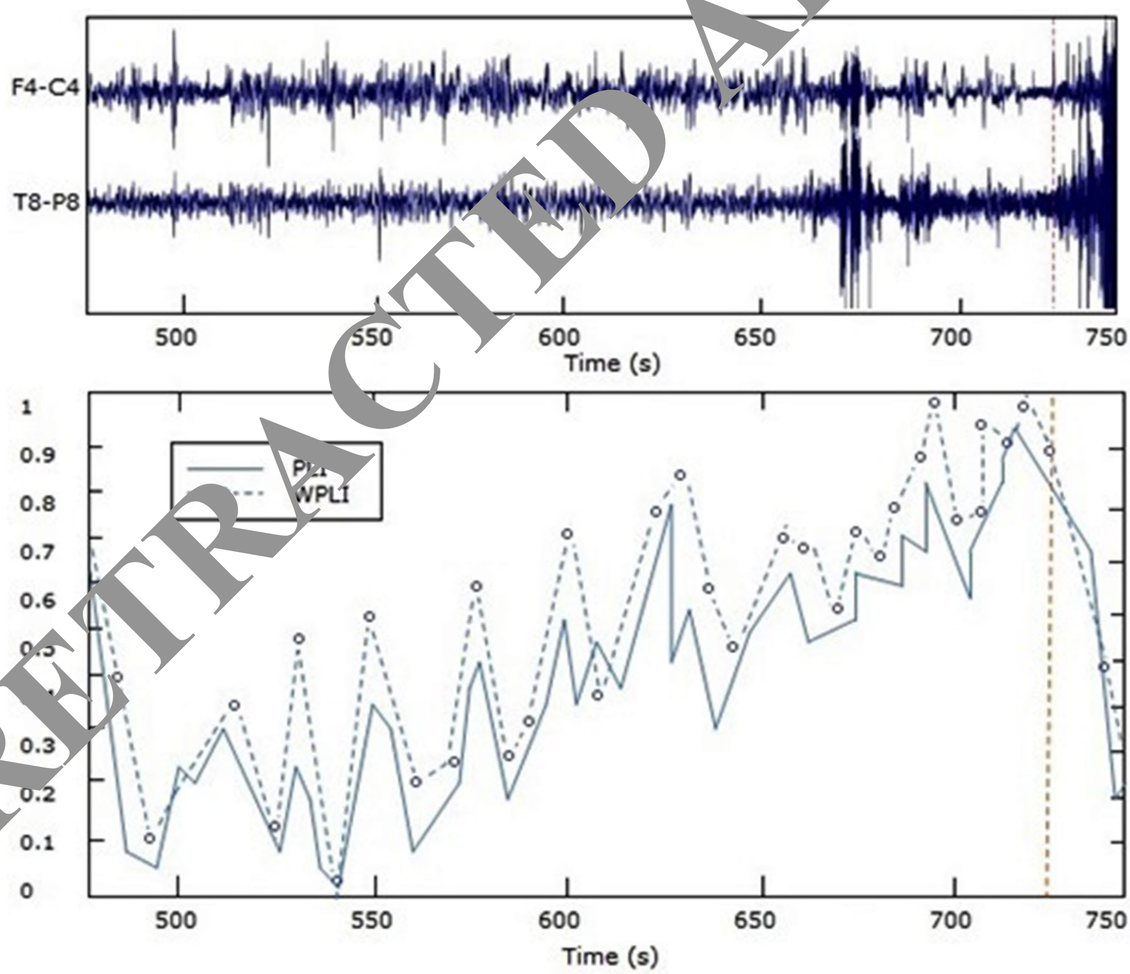

Fig. 2 EEG signal from last seizure of Chb_07, PLI and WPLI on channels $x = \{F4–C4\}$, $y = \{T8–P8\}$

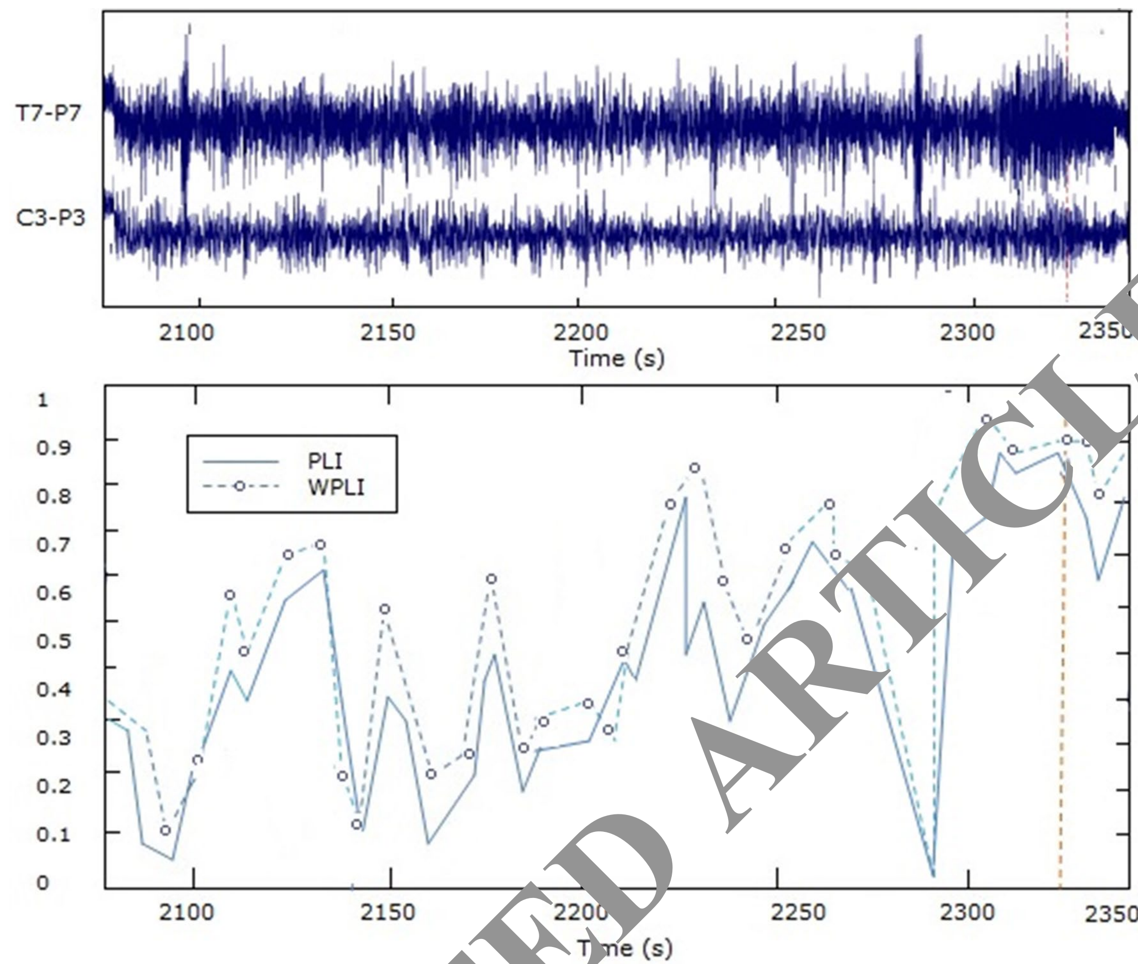

Fig. 3 EEG signal from second seizure of Chb_08, PLI and WPLI on channels $x = \{T7–P7\}$, $y = \{C3–P3\}$

where 'cp' gives Cauchy principal value. Therefore from the transform, the complex signal is constructed as

$$z(t) = a(t) + i\hat{a}(t) \; = \; X(t)e^{i\psi(t)}, \tag{2}$$

with $X(t) = \sqrt{[\hat{a}] \; + \; [a]^2}$ as amplitude and $\psi(t) = \arctan \frac{\hat{a}(t)}{a(t)}$ as phase.

Considering channels x and y, with Δ_t as time window incorporating N samples, the phase lock value (PLV) is detailed as follows from Eq. 3:

$$PLV_{x,y,\Delta t} = \left| \frac{1}{N} \sum_{q=1}^{N} e^{i\left|\psi_x(q) - \psi_y(q)\right|} \right|. \tag{3}$$

PLV portrays the average coherence among two signals regarding the angular distribution. It obtains closed interval values [0; 1], with the value '0' correlating to unsynchronized signals, while the value '1' correlating to complete synchronized signal. In recent past, the new measure has been popularized in Stam et al. (2007), namely phase lag index (PLI) for the measurement of functional connectivity in the brain region (Shah et al. 2018). The main conception centred on rejecting the difference that occurs in the phase which generally focused on '0' (mod 0). Thus, the increment and decrement in the short terms changes of synchronization measures can be studied. With the intention of elimination of the phase differences, an asymmetry index is elucidated by estimating the likelihood so that the phase difference $\Delta\psi$ will turn out to be in the range $(-\pi, \pi)$.

Considering the channel pairs x and y with the time window along with N instants, PLI is presented by Eq. 4:

$$PLI_{x,y,\Delta t} = \left| \frac{1}{N} \sum_{q=1}^{N} sign(\psi_x(q) - \psi_y(q)) \right| \tag{4}$$

where $\psi_x(q)$ and $\psi_y(q)$ are the phases of two signals on time instant q for channels x and y, respectively, influenced by the Hilbert transformation. It obtains closed interval values $0 \leq PLI \leq 1$, with the value '0' corresponding to no coupling or difference in phase generally focused on 0 (mod 0),

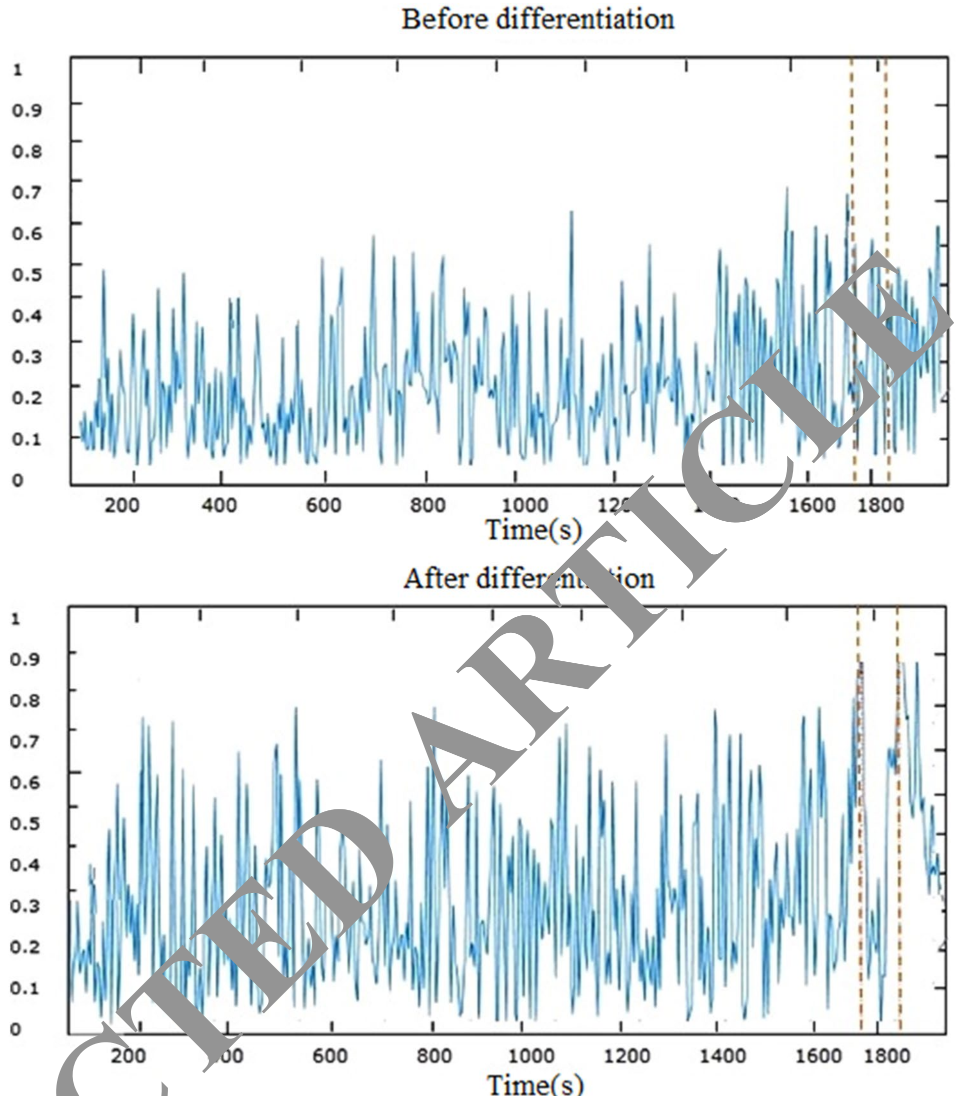

Fig. 4 Calculated WPLI with $x=\{P3–O1\}$ and $y=\{FT9–FT10\}$ on the fifth seizure of patient Chb_15, with and without differentiation

while the value '1' corresponds to a perfect phase locking when the phase difference occurs at a value. When the value of phase locking is stronger than non-zero values, PLI value will be larger.

The lack of coherence of PLI to narrow perturbations converts lags in phase into leads and contrariwise, as a result, an additional measure called weighted phase lag index (WPLI) has been founded in Park et al. (2011). This index value ranges within 0 and 1 and this can be provided as follows from Eq. 5:

$$\mathrm{WPLI}_{x,y,\Delta t} = \left| \frac{1}{N} \sum_{q=1}^{N} \frac{\left|\sin(\psi_x(q) - \psi_y(q)\right|}{\sin(\psi_x(q) - \psi_y(q)} \right| \quad (5)$$

Figures 2 and 3 represents the EEG signal of two different channels x and y over time in seconds for the seizure patient Chb_07 and Chb_08 from the EEG database are considered as examples. According to the lag's magnitude value, the phase difference is weighted. The phase difference which occurs near to the zero will lead to the WPLI calculation. This condition may contribute to increasing the sensitivity of the epileptic seizure prediction during phase synchronization and reduction of the false positive connectivity when phase synchronization is near to zero phases. Above calculated synchronization indices are not applied directly on the original signal, rather it is applied on the time-derivative value of the EEG signal.

This synchronization methodology has been used for the seizure prediction Parvez and Paul (2016). Two channels $x=\{P3–O1\}$ and $y=\{FT9–FT10\}$ are considered for WPLI. It has been concluded from the above work that WPLI rises at the starting time span of the seizure and appears as a peak at the outset of the seizure. To illustrate the importance of using the differential operator, Fig. 4 exhibits the extracted

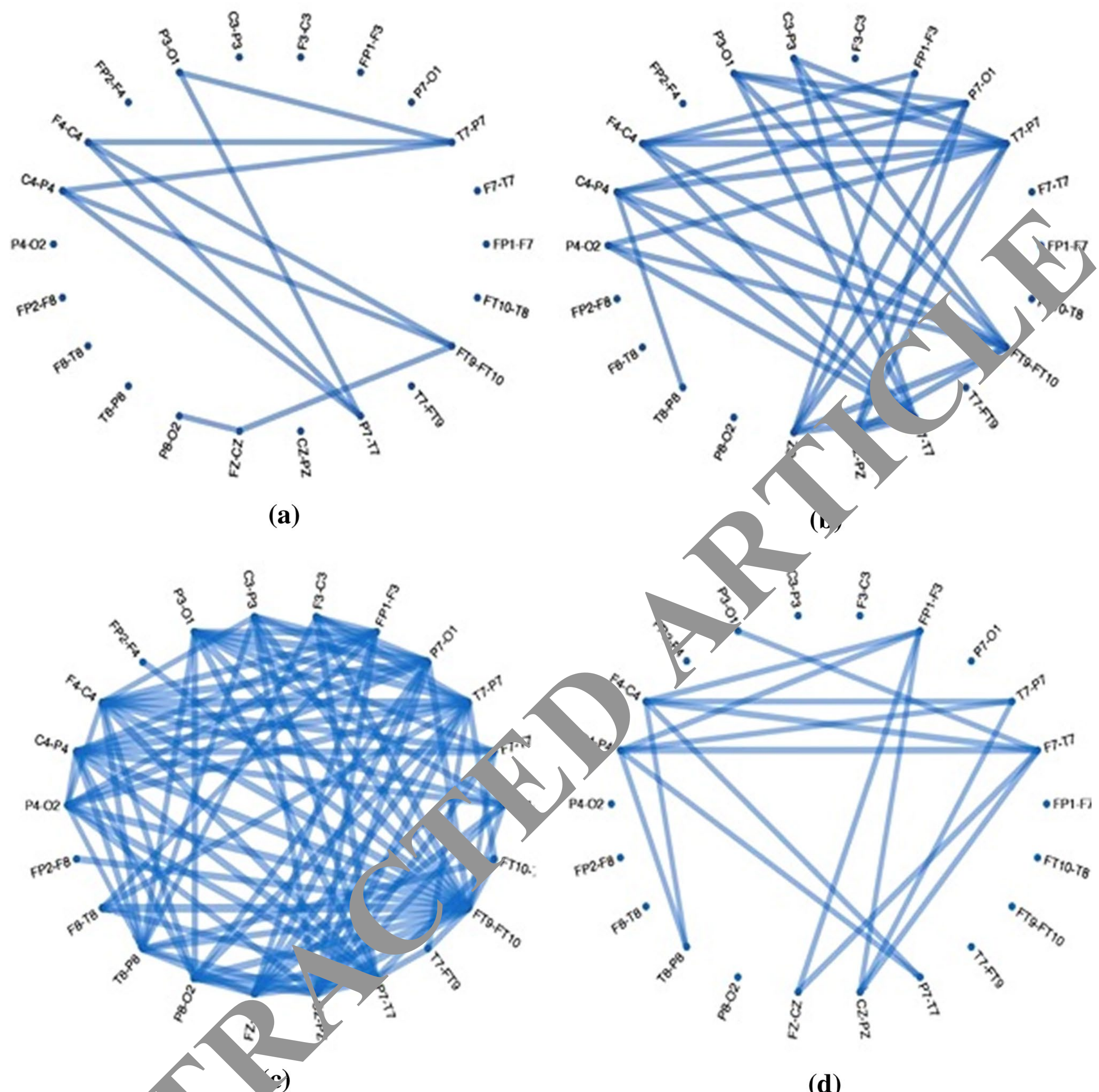

Fig. 5 **a** Δ_t = [405; 411] from G; **b** Δ_t = [415; 421] from G; **c** Δ_t = [425; 431] from G; **d** Δ_t = [420; 436]] from G

WPLI for the case Chb_15 with and without differentiation respectively.

2.4 Graph model of the brain functional connectivity measurement

The measured synchronization values are symmetric in nature therefore, it could be provided as $w_{x,y} = w_{y,x}$. From the previous works Rubinov and Sporns (2010) and Direito et al. (2011), it has been perceived that the relationship among the electrodes positioning on the scalp and their interconnections demonstrates the brain connectivity in-terms of the network model. Correspondingly brain network model can be constructed as an Undirected weighted graph, G = (V, X) where the nodes symbolise channels, and connection amongst the channels x and y are provides by an undirected weighted edge $(x, y) \in X$. Certainly, this Graph model provides a framework to construct reliable algorithms

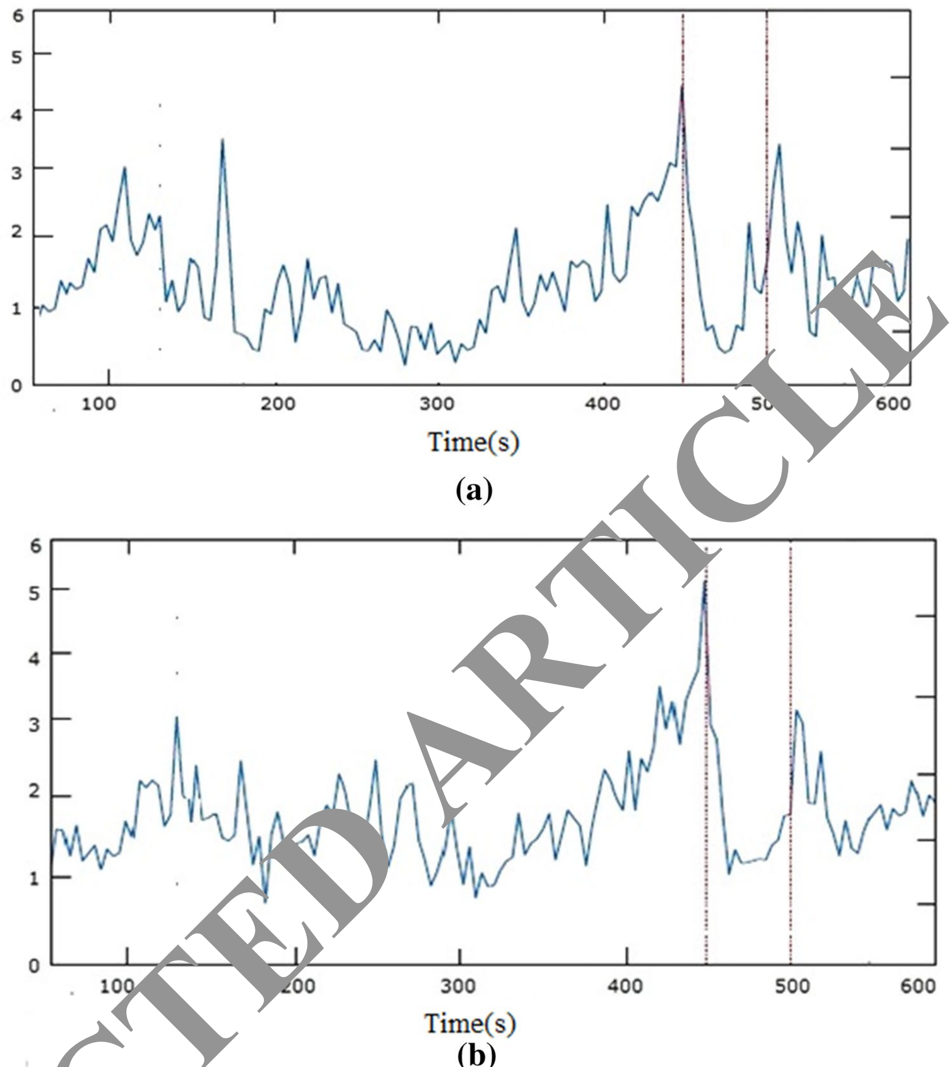

Fig. 6 **a** Node's strength {T7–P7}; **b** node's strength {P7–O1} for third seizure of Chb_07

for seizure prediction based on graph model significantly which may be used for synchronization measures. Node's degree can be employed to obtain the total count of connected edges to a node in graph G incorporating with a condition that weights could be larger than an actually provided threshold. Similarly, the strength of a node gives the total average of the weighted edges which are incident at graph G with a node (Alotaiby et al. 2017).

On account of the fact that Fig. 5 interpret the progression of the graph model at G with distinct instants in the advances of epileptic seizure prediction.

As an example, Chb_07 with the third seizure is chosen from the database, which starts at 432 s. The graphs which are provided are associated to a 6 s time window and the weighted edge quantifies the Phase lag index between two x and y channels from Eq. (2).For the appropriate view, edges that are larger than 0.9 are observed and the nodes are arrayed around the circle. The Highest weighted edges increase at two windows as shown in graphs from Fig. 5a–c, directly before the seizure are provided in Fig. 5d which implies an improvement in the synchronization. Figure 6a, b outlines the node's strength which is calculated by using PLI for channels P3–O1 and T7–P7 respectively on a 600 s time span comprising the record of third seizure for case Chb_07.

The two vertical dotted lines imply the ictal duration. It is noteworthy from the above statement there may be a hike for the upcoming ictal period, and then it decreases. The period right away the ictal period so-called pre-ictal period. From this study, the length between the pre-ictal periods is referred to as the prediction interval.

2.5 Featuring the deviation in the EEG synchronization

Even though the above-stated synchronization measures could be considered for classification problem.

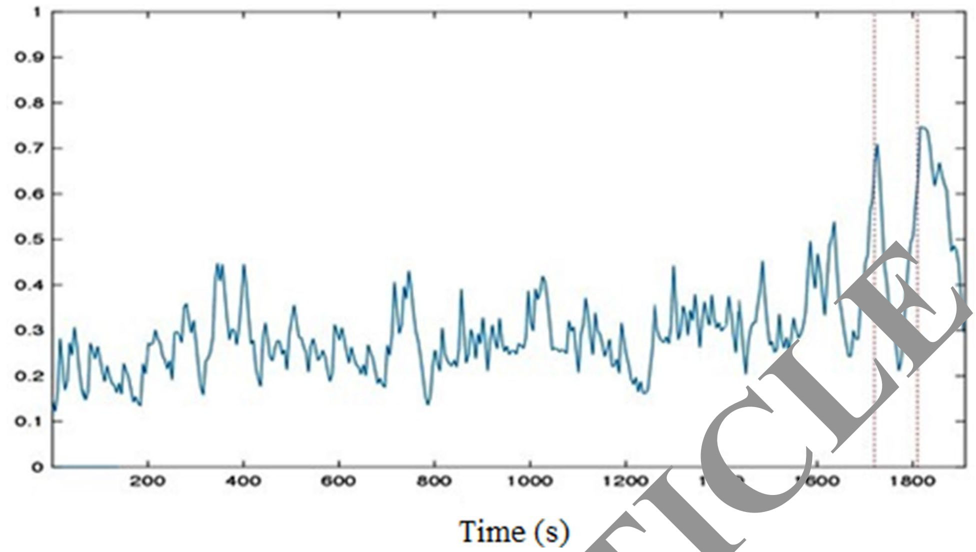

Fig. 7 MAACoD computed on WPLI with $x = \{FP3–O1\}$and $y = \{FT9–FT10\}$ for Chb_15

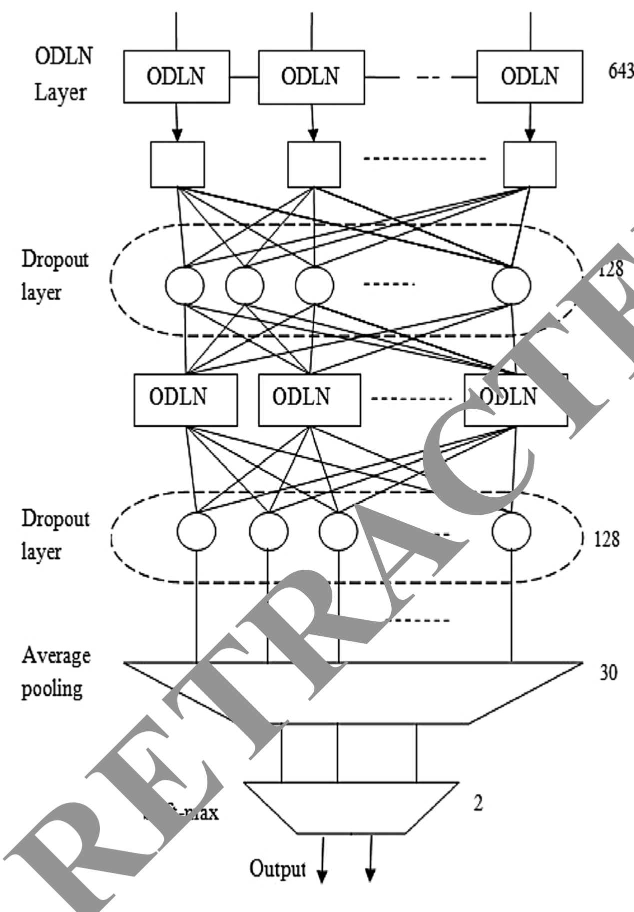

Fig. 8 Proposed ODLN_3 model

Despite that, the features can be integrated with the additional information derived from the synchronization calculations. To provide seizure prediction more accurately, it could be important to emphasize the rising inclination in the synchronization calculations which could be an indication for the occurrence of a seizure. To improve the rising inclination property for the extracted feature. The previously measured values of PLI and WPLI are herewith denoted as $f_{x,y}(\Delta t)$. Few functions are provided below:

2.5.1 Selection of the trend function:

A function $T_{x,y}(\Delta t)$ detailing the trends of the common feature $f_{x,y}(\Delta t)$ at time duration Δt. The representation of the trends is generally provided with reference to a weighted moving mean (WMM). In this work, the trend function $T_{x,y}(\Delta t)$ are selected as an EMA and it is formulated from the Eq. 6:

$$T_{x,y}(\Delta t) = \begin{cases} f_{(x,y)}(1) & \text{for } t = 1 \\ \left(\frac{2}{w+1}\right) f_{x,y}(\Delta t) + \left(1 - \frac{2}{w+1}\right) T_{x,y}(\Delta t - 1) & \text{for } t > 1 \end{cases} \quad (6)$$

From various trials, we have chosen $w = 8$ as an excellent trend seizure prediction.

2.5.2 Selection of the elevation function:

A function $E_{x,y}(\Delta t)$ detailing the elevation of the current inclination above the lower limit to detect whether an increasing inclination eventuates for an appropriate time interval. The idea brought about the trading indicator has been implemented, namely moving average convergence or divergence (MACoD). It provides the difference among moving averages for short and long time intervals. Often it has been confirmed that higher the trend, the moving average of short interval improves and vice versa for lower trend.

2.5.3 Selection of the appropriate lower limit:

A function $L_{x,y}(\Delta t)$ detailing the appropriate lower limit of $T_{x,y}(\Delta t)$ above in a time window to provide the current past in-terms of the time period is formulated from Eq. 7:

$$L_{x,y}(\Delta t) = \min_{\tau \in \{\Delta t - q, \ldots\ldots \Delta t\}} \{T_{x,y}(\Delta t)\} \tag{7}$$

Here, the value of q is chosen as $q=26$ for providing a required lower limit in seizure prediction application.

In this present work, it is predominant to analyze the specific rising trend for detecting the pre-ictal state, thus it has been concluded that improved performance is obtained by incorporating current lower limit to longer average period. This observation also comes out with an outbreak in finding the absolute information regarding the elevation in the amplitude over the present smaller amplitude value. These differences are known as moving average in amplitude convergence or divergence (MAACoD), calculated from the Eq. 8:

$$E_{x,y}(\Delta t) = T_{x,y}(\Delta t) - L_{x,y}(\Delta t) \tag{8}$$

Finally, the proposed MAACoD has been implemented for every measure $f_{x,y}(\Delta t)$, and provided as a feature for the classification. Figure 7 exhibits an example after implementing the MAACoD computed over the WPLI for Fig. 4. It can be noticed that MAACoD increases for the onset of the seizure.

3 ODLN model evaluation

To study the significant characteristics of the epileptic seizure from EEG data, deep learning was established to extract the differential features of EEG features that are associated with the prediction of seizures. A pre-analysis is carried out with three different models namely ODLN_1, ODLN_2 and ODLN_3.The simplest model namely OLDN_1 consists of single layer together with 32 memory units. In the ODLN_2 model, the number of memory units is increased to 128 units together with a single layer.An addition layer with the same 128 units the same as that of the previous dimension is incorporated in OLDN_3 as outlined in Fig. 8. This analysis is provided for learning the short -long term attachments among the same and different EEG data over the same class.

The fully connected layer was maintained as the next layer to transfer the knowledge obtained by the ODLN layer into meaningful seizure classification process. In this work, a fully connected layer is organized with 30 units utilizing the "Relu" the activation function (Chandaka et al. 2009). The output from this stage is transmitted through a one-dimensional layer so-called average pooling. It was adopted

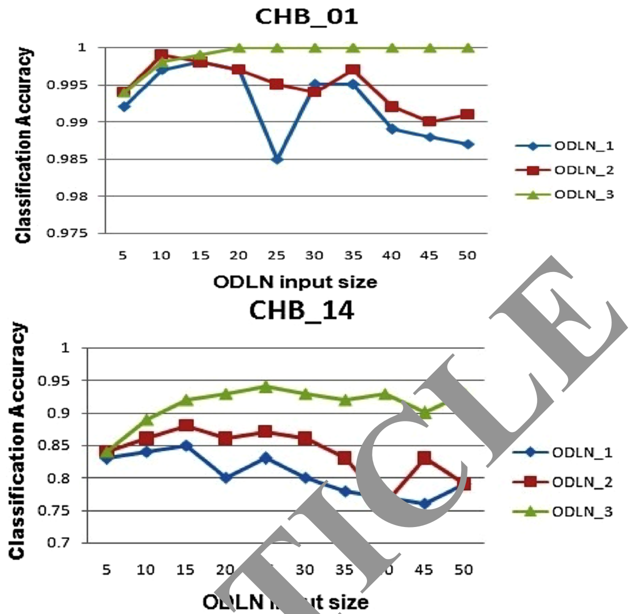

Fig. 9 Representing the classification accuracy for each network model per ODLN input size for Chb_01, and Chb_14

to contribute the equality in labelling the EEG segments for seizure prediction (Kumar and Kolekar 2014). The "Soft-max" layer is considered as a final layer to provide a label for the binary classification as Pre-ictal or inter-ictal. From an optimization interpretation, (Myers et al. 2016) Soft-max is considered as a commonly used function in machine learning to characterize a probability distributive function over the feature space.

In the proposed ODLN, the network was trained with "categorical cross-entropy" as the cost function with adaptive moment estimation so-called ADAM as an optimizer with batch size as '10'. The learning rate is assigned as 0.001, $\beta1=0.98$, $\beta2=0.100$, decay$=0.001$. The ODLN were implemented using Keras 2.0.9 [19] with Tensor flow 1.4.0 backend [20] worked on Python 3.6.

Chb_01and Chb_14 are randomly chosen to evaluate the proposed ODLN model for the CHB-MIT EEG database. The different pre-ictal time window is assigned from 15 to 120 min. Similarly, ODLN is evaluated with a size (input) of 643×5 and up to 643×50 features for the provided 50 EEG segments.

From the Fig. 9, the contribution of ODLN model for the classification accuracy is proved and it is figured out that except Chb_01 there would be margin variation less than 1%. Outcomes of this pre-analysis confirm the added advantage of implementing the two complex layer network so-called ODLN_3 contribute to the higher accuracy (Abadi et al. 2016). The mean variation for ODLN_1 model is also identified as 0.06% for 0.5 and 0.2 dropout rates, which influence the need of segment shuffling before the classifications

Table 2 The overall results for the pre-ictal window duration at 15 and 30 min for the 24 subjects of the CHB-MIT EEG database

Patient id	Window duration (15 min)					Window duration (30 min)				
	ODLN input size	EBE		SBE		ODLN input size	EBE		SBE	
		SEN (%)	FPR (h^{-1})	SEN (%)	SPEC (%)		SEN (%)	FPR (h^{-1})	SEN (%)	SPEC (%)
Chb_01	20	100	0	100	100	20	100	0	100	100
Chb_02	35	100	0	100	100	32	100	0	100	100
Chb_03	45	100	0.21	99.91	98.67	45	100	0	99.54	[illegible]
Chb_04	50	100	0.16	99.95	99.1	40	100	0.11	97.89	99.23
Chb_05	50	100	0.27	98.08	98.01	30	100	0.12	99.89	[illegible]
Chb_06	50	100	0.35	100	98.01	45	100	0.36	[illegible]	[illegible]
Chb_07	40	100	0	100	100	50	100	0	100	[illegible]
Chb_08	25	100	0.01	99.54	100	10	100	0	100	98.78
Chb_09	45	100	0.09	98.78	99.32	40	100	0	99.34	99.45
Chb_10	30	100	0	99.78	100	20	100	[illegible]	[illegible]	98.98
Chb_11	20	100	0	100	100	20	100	0	100	100
Chb_12	40	100	0	100	99.89	25	100	0	99.67	100
Chb_13	45	100	0	91.12	95.78	30	100	[illegible]	100	99.98
Chb_14	35	100	0.68	98.45	98.83	50	[illegible]	[illegible]	95.65	98.23
Chb_15	45	100	0.13	100	99.72	45	100	0.19	98.34	99.12
Chb_16	30	100	0.1	100	100	50	[illegible]	0.05	99.05	99.78
Chb_17	30	100	0	99.13	99.13	15	100	0	99.34	100
Chb_18	50	100	0.13	100	100	25	[illegible]	0.02	99.67	99.89
Chb_19	20	100	0	100	99.68	30	100	0	100	100
Chb_20	20	100	0	100	100	[illegible]	100	0	100	100
Chb_21	45	100	0.06	100	100	[illegible]	100	0	99.65	100
Chb_22	40	100	0	99.68	[illegible]	[illegible]	100	0	100	100
Chb_23	25	100	0	99.21	[illegible]	45	100	0.05	100	100
Chb_24	40	100	0.25	[illegible]	[illegible]	30	100	0.12	99.23	99.78
Average		100	0.101667	[illegible]	[illegible]		100	0.069583	99.40375	99.63125

make the non-requirement of dropout layer (Aarabi et al. 2009). In accordance with the above outcomes, ODLN_3 model will be finally adopted in this [illegible] and from here it is referred to as simply ODLN model constructed without dropout layer.

4 Results

The synchronization measures are calculated using the PLV, PLI, and WPLI and it has been concluded that WPLI increases at the onset of the pre-ictal duration of the seizure. Furthermore, for obtaining the seizure prediction it might be predominated to mark the rising trend in the synchronization measures for predicting the pre-ictal seizure state. Finally, the proposed MAACoD has been implemented for every measure of the EEG segment, and an increases for the outset of the pre-ictal seizure state is observed. With the intention of strengthening the accuracy evaluation results, event-based evaluation (EBE) and segment-based evaluation (SBE) are employed.

4.1 Patient-specific ODLN input size evaluation

The four pre-ictal time windows are used namely 15, 30, 60 and 120 min with various inputs EEG segment size to the ODLN network which are assessed for each subject of the EEG database. From Tables 2 and 3, illustrates the importance of the ODLN input size for obtaining minimal false prediction rate (FPR) per pre-ictal time window along with its performance metrics.

4.1.1 Event based evaluation (EBE)

The results obtained from Tables 2 and 3, effectively detects the seizure for all pre-ictal time windows, maintain 100% sensitivity on average. The FPR is consolidated with 0.069 FP/h for 30 min pre-ictal window when compared with 0.101 Fp/h for 15 min time window.

Table 3 The overall results for the pre-ictal window duration at 60 and 120 min for the 24 subjects of the CHB-MIT EEG Database

Patient id	Window duration (60 min)					Window duration (120 min)				
	ODLN input size	EBE		SBE		ODLN input size	EBE		SBE	
		SEN (%)	FPR (h^{-1})	SEN (%)	SPEC (%)		SEN (%)	FPR (h^{-1})	SEN (%)	SPEC (%)
Chb_01	20	100	0	100	100	15	100	0	100	100
Chb_02	35	100	0	100	100	20	100	0	100	100
Chb_03	45	100	0	99.12	99.89	20	100	0	100	100
Chb_04	50	100	0.06	99.86	99.78	30	100	0	99.89	99.89
Chb_05	45	100	0	99.67	100	50	100	0	99.67	100
Chb_06	50	100	0.16	99.05	98.87	45	100	0.14	99.98	[illegible]
Chb_07	45	100	0.01	100	99.86	45	100	0.05	100	99.78
Chb_08	35	100	0	100	100	30	100	0	99.87	100
Chb_09	25	100	0.02	99.56	99.89	30	100	0	100	100
Chb_10	45	100	0.04	98.09	99.89	20	100	[illegible]	99.89	99.89
Chb_11	20	100	0	100	100	40	100	0	100	100
Chb_12	15	100	0	100	100	35	100	0	99.87	100
Chb_13	40	100	0	100	100	40	100		99.91	100
Chb_14	50	100	0.3	98.89	98.08	50	100	[illegible]	98.78	99.78
Chb_15	35	100	0.24	99.04	99.87	40	100	0	99.76	100
Chb_16	20	100	0	99.78	100	15	100	0.05	99.89	100
Chb_17	40	100	0	100	100	40	100	0	99.56	100
Chb_18	45	100	0.05	99.46	99.87	35	100	0.09	99.98	99.67
Chb_19	45	100	0	100	100	40	100	0	100	100
Chb_20	10	100	0	100	100	5	100	0	100	100
Chb_21	35	100	0	99.67	100	[illegible]	100	0	100	100
Chb_22	45	100	0	99.95	100	40	100	0	100	100
Chb_23	30	100	0	100	100	15	100	0	100	99.98
Chb_24	45	100	0	100	99.78	30	100	0.05	100	99.78
Average		100	0.036667	[illegible]	[illegible]		100	0.020833	99.87708	99.94792

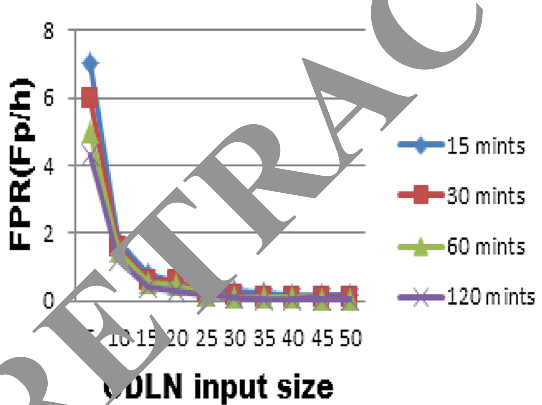

Fig. 10 Mean values of FPR per ODLN input size for all 24 subjects

Along with it, at 15 min pre-ictal time window 12 out of 24 subjects found to have 100% sensitivity with zero FPR and at 30 min pre-ictal time window 13 out of 24 subjects come up with 100% sensitivity with zero FPR. It is also observed that increasing the pre-ictal time window, the FPR reduces further as 0.036 for 60 min, and 0.020 for 120 min. Similar the zero FPR are detected as 16 and 17 out of 24 subjects for 60 min, and 120 min pre-ictal time window respectively with 100% sensitivity. Finally, it has been concluded that the increase in the pre-ictal time window improves the accuracy of seizure prediction rate with more zero false alarms.

4.1.2 Segment based evaluation (SBE)

The classification for the EEG signals utilizing the 15 min pre-ictal time window provides a mean sensitivity and specificity of 99.31% and 99.35% respectively. Similarly, the 30 min pre-ictal window provides a mean sensitivity and specificity of 99.40% and 99.63% respectively. Furthermore, the highest accuracy rate among the four-time window is found at 120 min pre-ictal window with sensitivity and specificity as 99.87% and 99.94% correspondingly.

Table 4 Comparison with few published studies that used the CHB-MIT EEG database

Study	Features	Classifier	SEN (%)	SPEC (%)	FPR (h^{-1})
Aarabi et al. (2009)	Spectral power	BNN	91.0	95.0	–
Chandaka et al. (2009)	Cross correlation	SVM	92	100	–
Kumar and Kolekar (2014)	Fractal dimension	SVM	98.0	96.0	–
Myers et al. (2016)	PLV	SVM	77	–	0.17
Alotaiby et al. (2017)	Common spatial pattern statistics	LDA	89	61	0.47

4.2 Global ODLN input size evaluation

It is necessary to determine the probable global number of EEG segments used for evaluating the ODLN model from the preanalysis of ODLN input size. From the above section, it is confirmed that the FPR is firmly varied by the input size of ODLN. Figure 10 demonstrates the relationship between the ODLN input size and FPR as they are inversely proportional to each other. It is also important to notice that only at 15-min pre-ictal window, FPR rate is larger than 0.125 Fp/h which provides three false alarms in a day.

In addition to it, this could be taken into account as a quantitative threshold of seizure prediction performance. So, it proves that ODLN input size larger than 35 may provide FPR less than 0.125 Fh/p for next pre-ictal time windows. Examining the variation of segment-based evaluation, it could be concluded there may be 0. 2% variation occurs for the 30–45 ODLN input size, in both sensitivity and specificity. Therefore, the optimal number of selection of EEG segments within this range is predicted to maintain closely identical performance.

5 Discussion

The interpretation outcomes of the proposed seizure classification approach are able to anticipate all 185 seizures subjects of the database with a very low false alarms rate per hour of EEG signals. Tables 2 and 3 exhibits that the schemed ODLN model is able to provide a low false alarm ranging from 0.10–0.02 Fp/h, shows that the increase in the pre-ictal time window decreases the FPR. Besides zero FPR could be able to observe for 12–17 subjects out of the 24 subjects from the database based on the duration of the pre-ictal time window, indicate that seizure prediction is very error-free with little FPR. This performance rate could be maintained only if the EEG segment is maintained on average of 30–45 EEG segments as an input to ODLN model.

It is confirmed from the evaluation result that a false alarm rate is perpetually occurring around 0.036–0.151. Furthermore, the FPR rate reduces from 0.101 to 0.020 Fp/h with the increase in the time window from 15 to 120 min, witnessed with increased performance rate. Table 4 provides a comparison of the proposed model with other classification approaches of previous works.

The proposed ODLN classifier is capable of contributing more appropriate seizure prediction performance than any of the previous approaches. As mentioned, the proposed work is introduced to optimize the deep learning for LSTM networks over convolutional neural networks (CNN) that have been considered for seizure prediction in literature with EEG application. This work can be extended with different time window in multiple times which would help to predict seizures with reduced false alarm.

6 Conclusion

The deep learning algorithms effectuate their potentiality in managing the complex nature of EEG data in demanding biomedical applications like seizure prediction, sleep stage prediction, etc. Therefore, ODLN (optimized deep learning network) were introduced in this research work and validated as a useful tool for the pre-ictal EEG signals. Intending to assess the synchronization measures from the EEG signal, PLI, WPLI, and graph model was considered. Furthermore, MAACoD is measured to identify the highlights in the synchronization patterns. The ODLN model is developed to classify the pre-ictal and ictal states based on the pre-ictal window. Future work of this proposed work includes modifying the ODLN model to incorporate multi-channel EEG systems with different pre-ictal window duration.

References

Aarabi A, FazelRezai R, Aghakhani Y (2009) A fuzzy rule-based system for epileptic seizure detection in intracranial EEG. Clin Neurophysiol 120:1648–1657

Abadi M, Agarwal A, Barham P, Brevdo E, Chen Z, Citro C (2016) Tensorflow: large-scale machine learning on heterogeneous distributed systems. arXiv preprint. arXiv:1603.04467

Alotaiby TN, Alshebeili SA, Alotaibi FM, Alrshoud SR (2017) Epileptic seizure prediction using CSP and LDA for scalp EEG signals. Comput Intell Neurosci. https://doi.org/10.1155/2017/1240323

Appel G (2005) Technical analysis power tools for active investors. Financial Times Prentice Hall, New York **(ISBN 0-13-147902-4)**

Ashokkumar SR, MohanBabu G, Anupallavi S (2019) A KSOM based neural network model for classifying the epilepsy using adjustable analytic wavelet transform. Multimed Tools Appl. https://doi.org/10.1007/s11042-019-7359-0

Chandaka S, Chatterjee A, Munshi S (2009) Cross-correlation aided support vector machine classifier for classification of EEG signals. Expert Syst Appl 36:1329–1336

Cui S, Duan L, Qiao Y, Xiao Y (2018) Learning EEG synchronization patterns for epileptic seizure prediction using bag-of-wave features. J Ambient Intell Human Comput. https://doi.org/10.1007/s12652-018-1000-3

Deckers C (2003) Current limitations of antiepileptic drug therapy: a conference review. Epilepsy Res 53(1–2):1–17

Deivasigamani S, Senthilpari C, Yong WH (2020) Machine learning method based detection and diagnosis for epilepsy in EEG signal. J Ambient Intell Human Comput. https://doi.org/10.1007/s12652-020-01816-3

Direito B, Ventura F, Teixeira C, Dourado A (2011) Optimized feature subsets for epileptic seizure prediction studies. In: Engineering in medicine and biology society, EMBC, annual international conference of the IEEE

Fisher R, Salanova V, Witt T, Worth R, Henry T, Gross R (2010) Electrical stimulation of the anterior nucleus of thalamus for treatment of refractory epilepsy. Epilepsia 51:899–908

Hu W, Cao J, Lai X, Liu J (2019) Mean amplitude spectrum based epileptic state classification for seizure prediction using convolutional neural networks. J Ambient Intell Human Comput. https://doi.org/10.1007/s12652-019-01220-6

Iasemidis LD, Shiau DS, Pardalos PM, Chaovalitwongse W, Narayanan K, Prasad A (2005) Long-term prospective on-line real-time seizure prediction. Clin Neurophysiol 116:532–544

Kumar A, Kolekar MH (2014) Machine learning approach for epileptic seizure detection using wavelet analysis of EEG signals. In: Proceedings of the MedCom'2014. IEEE, pp 412–416

Le Van Quyen M, Navarro V, Martinerie J, Baulac M, Varela FJ (2003) Toward a neurodynamical understanding of ictogenesis. Epilepsia 44(12):30–43

Mormann F, Kreuz T, Rieke C, Andrzejak RG, Kraskov A (2005) On the predictability of epileptic seizures. Clin Neurophy 116:569–587

Myers MH, Padmanabha A, Hossain G, de Jongh Curry AL, Blaha CD (2016) Seizure prediction and detection via phase and amplitude lock values. Front Hum Neurosci 10:80

Ni Z, Yuksel AC, Ni X, Mandel MI, Xie L (2017) Confused or not confused? Disentangling brain activity from EEG data using bidirectional LSTM recurrent neural networks. In: Presented at the Proceedings of the 8th ACM international conference on bioinformatics, computational biology, and health informatics ,Boston, Massachusetts, USA

Park Y, Luo L, Parhi KK, Netoff T (2011) Seizure prediction with spectral power of EEG using cost-sensitive support vector machines. Epilepsia 52:1761–1770

Parvez MZ, Paul M (2016) Epileptic seizure prediction by exploiting spatiotemporal relationship of EEG signals using phase correlation. IEEE Trans Neural Syst Rehabil Eng 24(1):158–168

Ramgopal S, Thome-Souza S, Jackson M, Kadish NE, Fernandez IS, Klehm J (2014) Seizure detection, seizure prediction, and closed-loop warning systems in epilepsy. Epilepsy Behav 37:291–307

Rubinov M, Sporns O (2010) Complex network measures of brain connectivity: uses and interpretations. Neuroimage 52(3):1059–1069

Sathyanarayana S, Satzoda RK, Sathyanarayana S, Thambipillai S (2018) Vision-based patient monitoring: a comprehensive review of algorithms and technologies. J Ambient Intell Human Comput 9(2):225–251

Shah SA, Fan D, Ren A, Zhao N, Yang X, Tanoli SAK (2018) Seizure episodes detection via smart medical sensing system. J Ambient Intell Human Comput. https://doi.org/10.1007/s12652-018-1142-[illegible]

Shoeb A, Guttag J (2010) Application of machine learning to epileptic seizure detection. In: Proceedings of the 27th international conference on machine learning (ICML '10), Haifa, Israel, pp 975–982

Stam CJ, Nolte G, Daffertshofer A (2007) Phase lag index: assessment of functional connectivity from multi channel EEG and MEG with diminished bias from common sources. Hum Brain Mapp 28:1178–1193

Vinck M, Oostenveld R, Van Wingerden M, Battaglia F, Pennartz C (2011) An improved index of phase-synchronization for electrophysiological data in the presence of volume-conduction, noise and sample-size bias. Neuroimage 55(4):1548–1565